Image-guided surgery of liver metastases by three-dimensional ultrasound-based optoelectronic navigation

Author: Brian Jensen

Seminar in Computer Aided Surgery
Chair for Computer Aided Medical Procedures & Augmented Reality, Department of Informatics, TU München
Supervisor: Tobias Blum
Advisor: Prof. Dr. Nassir Navab

Patients diagnosed with primary liver carcinomas or secondary metastases from colorectal carcinomas are often associated with a very slim prognosis. Currently the only treatment method with curative abilities is liver resection surgery. The highly morphological nature of the liver and its vascular structure make it difficult to properly assess possible resection strategies. Advanced preoperative image processing and visualization tools are needed to aid surgeons in preparing more aggressive surgical plans while at the same time allowing more of the functional liver tissue to be preserved. This paper discusses several methods for computer aided liver resection and is based upon an experiment conducted on their application [2].

1 Background Information on Liver Metastases

The term cancer is used to designate a group of cells that exhibit the following symptoms: uncontrolled growth, invasion or destruction of adjacent tissues, and sometimes metastases. A metastasis is a cancerous growth from an existing tumor that has spread to a new location in the body. Cancer of the liver is an ultimately fatal disease if left untreated, with the average survival period lasting from 3 to 6 months [7]. Liver cancer can be caused either by a primary malignant tumor manifestation, known as hepatocellular carcinoma, or the result of metastasis from another site, typically from the colorectal region.

$$\begin{pmatrix} a_1 & a_2 & a_3 \\ b_1 & b_2 & b_3 \\ c_1 & c_2 & c_3 \end{pmatrix}$$

In the western world, where hepatitis infections are seldom, most occurrences of a liver carcinoma are metastases from other tumors. Colorectal cancer is the third most common form of cancer in human beings. About one third of the patients with colorectal cancer will

develop metastases in the liver. The median survival rates for untreated hepatic metastases spans from 7 to 10 months, which vary based upon the severity of the hepatic involvement [1].

1.1 Methods of Treatment

Although there are several methods of treatment available for liver metastases, only one has the potential to be curative. Studies have shown that of three chemotherapy approaches to treating the liver metastases, none offered a significant increase in survival rates, with the median being 10 to 13 months, and few surviving longer than a two year period [6]. A liver transplant would be a theoretical treatment, although the procedure is not performed in patients with liver metastases, mostly because of the high reoccurrence rate of the metastases. The only method with the possibility for a long term cure for such patients is liver resection surgery.

1.2 Liver Resection

Liver resection surgery involves removing lobes of the liver containing malignant tissue, while preserving the overall function of the liver as a whole. The liver is a unique organ in the human body due to its ability to regenerate itself, assuming enough functional tissue is remaining. It has been shown that 70 - 80% of a healthy non cirrhotic liver can be resectioned, when there are enough blood supply and drainage vessels left over to supply the remaining tissue [13].

The most important factor in achieving a positive long term outcome of liver resection surgery is a resection with a negative margin $R0$ [4]. In resective surgery a negative margin, labeled as $R0$, indicates the margin or edges of the removed tissue has been examined by a pathologist and contains no malignant tissue. It is therefore critical to the success of the operation that the surgeon can guarantee a negative margin while still leaving enough tissue intact to prevent liver failure.

In order for resection to even be considered as treatment for liver metastases a few conditions have to be met. Foremost, the primary cancer site has to be treatable with a positive prognosis. Additional metastases in other organs need to be ruled out. Beyond this the liver needs to be in a moderately healthy state and free of cirrhosis. Liver cirrhosis designates a damaged state of the liver tissue, often caused by alcoholism or by hepatitis infections, that severely detriments the function of the liver and its regenerative abilities. Cirrhosis hinders the successful regeneration of the resected tissue while increasing the risk of complete liver failure.

Although a patient may fulfill the general requirements for a resection does not mean that the procedure can be performed. A lot depends upon the exact location and amount of tumors. Liver metastases tend to form in multiple locations in the liver, usually in difficult to access locations deep inside the liver around major vessels. This complicates the assessment of resection viability because the surgeon has to evaluate how much liver tissue has to be removed to ensure a negative margin, and how much tissue can be supported by the remaining blood vessels.

1.2.1 Classic Resection Approach

The liver is a somewhat complicated organ because its vascular anatomy can vary from patient to patient. In general the liver has four main vessel systems that provide blood supply and

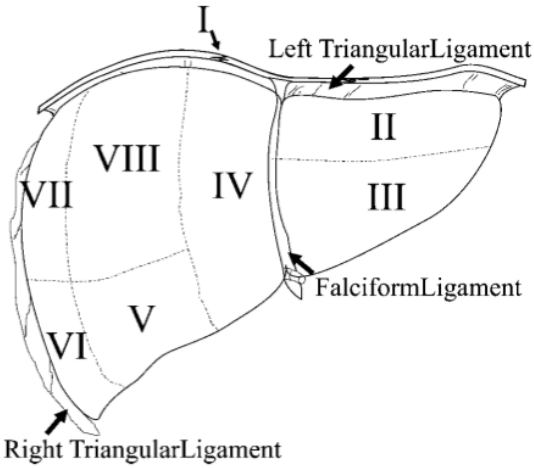

Figure 1: This figure depicts the Couinaud scheme for liver vascularization. Each of the 8 sections can be removed without damaging the vascularization of the others.

drainage, the portal vein, the hepatic vein, the hepatic artery, and the bilary ducts. Any resection needs to guarantee that the remaining liver tissue is adequately supplied by these four systems in order to be successful. The vascular system of the liver does follow a pattern though, as the hepatic vein and the bilary ducts run parallel to the portal vein. Because of this feature, the portal vein is used as the main identifier for determining the vascularization of different areas of the liver.

Nonetheless, it is still very difficult for a surgeon to picture the three dimensional layout of the various branches of the portal vein just by analyzing two dimensional slices of a CT or MR scan. Determining which branches of the portal vein would be affected by a planned resection using this method is very impractical and prone to error. Assuring that the remaining tissue after resectioning is properly vascularized, is nearly impossible.

To ease this problem a schematic model of the liver was proposed by Couinaud [3]. In this model the liver is divided up into 8 different segments, see figure 1. Each of these segments are independently supplied by a third order branch of the portal vein, and thus can be removed without adversely affecting any of the other segments. Using this model the surgeon needs to only determine in which segments that the tumors lie in order to calculate out the remaining liver volume, assuming all metastases were correctly diagnosed.

1.2.2 Compuer Aided Resection Planning

The Couinaud model is a very simplistic view of the vascularization of the liver because of its assumptions that the liver anatomy is roughly the same in all patients. This poses problems as research has shown that this is not necessarily true, the amount, size or position of these segments can be extremely variable from patient to patient. One direct consequence of this is that preoperative resection plans sometimes have to be modified during the operation, when the surgeon detects that certain tissue is unexpectedly at risk for devascularization.

More desirable is the construction of an individual vascular map for each patient, so that the surgeon can plan a more aggressive surgery while at the same time reducing the amount of liver tissue that needs to be resected. Using advanced image processing techniques, the entire

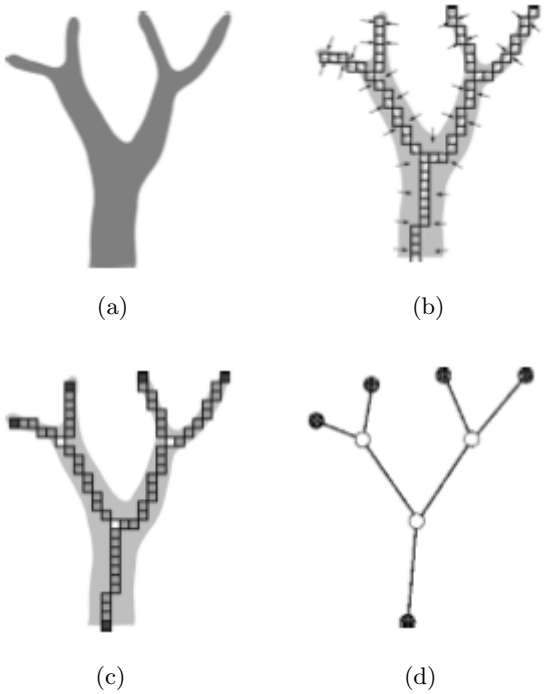

Figure 2: This shows the four processing steps necessary to analyze the vascularization properly. Beginning with the segmented vessels (a), a skeleton is generated using advanced thinning (b), then the ramification points are marked (c), and finally a graph is produced (d).

vascular structure of the liver can be segmented and then visualized in three dimensions. In addition to displaying the vascular structure, individual vascular supply areas, similar to the segments used in the Couinaud model, can be calculated, providing a higher level of accuracy for presurgical planning. The benefit of using these tools over standard preoperative planning methods is that they allow the resected liver volume to be calculated more accurately, thus decreasing the risk that the liver remnant is too small to function [9].

2 Preoperative Surgical Planning

2.1 Diagnostic Methods

Typically a contrast enhanced CT or MR scan is used as the primary diagnostic imaging modality. This is usually accompanied by a manual ultrasound scan, because sometimes the tumor sites do not show up properly in the CT or MR image. Most contrast agents involved show high intensity values for both the portal and hepatic veins, so these structures easily discernible in the images, a property we will use in preoperative image processing steps in the next section.

2.2 Image Processing

The necessary image processing that needs to be carried out can be broken down into three separate tasks. First the blood vessels need to be segmented from the rest of the liver voxels. Then the segmented voxels need to be ordered into an acyclic direct graph representing each individual vessel system. Finally the vascularization areas need to be determined using the graph. The methods used in this section were taken from [12].

2.2.1 Vessel Segmentation

The task of segmenting the vessel systems is accomplished using a modified thresholding based region growing algorithm. The technique used is summarized in algorithm 1.

Algorithm 1 Efficient Vessel Segmentation with Automatic Threshold Selection

1: {**INPUT: Voxel seed** beg**, selected manually close to the portal vein's entrance in the liver, and absolute lower threshold** Θ_{end}**}**
2: **{OUTPUT: Voxel Lists** $L(\Theta_{beg})$ **...** $L(\Theta_{opt})$**}**
3: $\Theta_{beg} =$ **Intensity value of** $begin$;
4: $L(\Theta_{beg+1}) = beg$; **{Initial Voxel List for** Θ_{beg}**}**
5: **for** $level = \Theta_{beg};\ level > \Theta_{end};\ level--$; **do**
6: **for all** $voxel \in L(level+1)$ **do**
7: **for all** $neighbor$ **from** $voxel$ **do**
8: **if** $\Theta_{neighbor} \geq level$ **then**
9: $L(level) \leftarrow neighbor$; **{Add the neighbor to our list for the current level}**
10: **end if**
11: **end for**
12: **end for**
13: **end for**
14: **{Find optimal lower Threshold** Θ_{opt}**, so that no liver tissue is segmented.}**
15: $\Theta_{opt} = \Theta_{end} + 1$;
16: **while** $CC_{left} + CC_{right}$ **not maximum do**
17: $\Theta_{opt}++$;
18: **end while**
19: **{Using the following definitions}**
20: $N(\Theta_{lev}) = |L(\Theta_{lev})| + ... + |L(\Theta_{begin})|$ **{Number of Voxels segmented at threshold}**
21: $CC_{left} =$ **Cross correlation of the line** $\frac{N(\Theta_{end}) - N(\Theta_{opt})}{\Theta_{end} - \Theta_{opt}}$;
22: $CC_{right} =$ **Cross correlation of the line** $\frac{N(\Theta_{opt}) - N(\Theta_{beg})}{\Theta_{opt} - \Theta_{beg}}$;

The algorithm takes a seed voxel, selected interactively with a location near the entrance of the portal vein into the liver, and an absolute lower threshold, which should be near the intensity values of normal liver tissue. The optimal lower threshold is calculated automatically. This is based on the observation that the amount of voxels segmented grows linearly from the starting voxel until the optimal lower threshold is reach. After the optimal lower threshold is reached the amount of voxels segmented grows at a much higher rate, because normal liver voxels start being segmented. These two growth rates can be estimated by creating two lines, one line through the points $(\Theta_{end}, N(\Theta_{end}))$ and $(\Theta_{opt}, N(\Theta_{opt}))$, the other through the the

points $(\Theta_{opt}, N(\Theta_{opt}))$ and $(\Theta_{beg}, N(\Theta_{beg}))$. The optimal threshold is found when the cross correlation of the two lines is maximum.

2.2.2 Seperation of Vessel Systems

The newly segmented vessel systems are still not in a suitable form that can be used to determine vascularization areas. Most preoperative images are produced using contrast enhancing substances that target more than one vessel system, causing each to have intensity voxels in the image. Because of the limited spatial resolution in the images, these voxels will appear adjacent to each other, and thus be segmented as one object, when in fact there is a separation between the two. Manual isolation of the vessel systems would be extremely time consuming and nearly impossible, instead the vessels and their branches will be identified using methods from graph theory. The four main steps involved in this process are visualized in figure 2.

The first step involves so called skeletonization of the segmented voxels. This process reduces the segmented voxels to a graph like wire frame that represents their shape and topology. Normally this would be achieved by constructing all lines that are equidistant from at least two points on all the boundaries, but this approach leaves gaps or adds irrelevant surfaces when used on discrete images. Instead an algorithm known as thinning is used to wear away the outer lying voxels until only a skeleton remains. The idea behind this can be seen in algorithm 2.

Algorithm 2 Fast 3D Skeletonization using Thinning

1: {**INPUT: Binary image** I **containing the segmented voxels**}
2: **{OUTPUT: Skeleton image** S**}**
3: $S = I$; **{Start off with binary image}**
4: $\Omega = \{Up, Down, North, South, East, West\}$; **{Direction to check for neighbors}**
5: **repeat**
6: $List_{delete} \leftarrow \varnothing$;
7: $voxelsDeleted = 0$;
8: **for all** $direction \in \Omega$ **do**
9: **for all** $voxel \in S$**, where** $voxel > 0$ **do**
10: **{Check if** $voxel$ **is an edge in the current** $direction$**}**
11: **if** $voxel$ **is border point for** $direction$ **in image** S **then**
12: **if** $voxel$ **is a simple voxel and not an endpoint in** S **then**
13: $List_{delete} \leftarrow voxel$; **{voxel is candidate for deletion}**
14: **end if**
15: **end if**
16: **end for**
17: **for all** $voxel \in List_{delete}$ **do**
18: **if** $voxel$ **is still simple and not an endpoint in** S **then**
19: $S(voxel) = 0$; **{Make sure topology doesn't change before deleting}**
20: $voxelsDeleted++$;
21: **end if**
22: **end for**
23: **end for**
24: **until** $voxelsDeleted = 0$

The algorithm expects a binary map where all segmented voxels are set to 1 and all others to 0 as input. It works by successively wearing down the borders of all shapes in the image in each direction. In each iteration it gathers all border voxels, makes sure they are not part of an end point, and then checks if the current voxel is a simple voxel. A simple voxel is a voxel whose removal does not change the topology of the image. If none of these conditions fail, the voxels are then added to the delete list, and not immediately removed, to prevent changes to image while further voxels are investigated. After all voxels have been visited, all voxels in the delete list are removed from the image. The conditions used in judging whether any given voxel is a simple voxel are beyond the scope of this paper, but can be found in [11].

Having a skeleton based representation of the different vessel systems has many advantages over the voxel based representation. On the one hand access to geometrical information such as vessel radius is easier, while on the other hand determination of structural information such as ramification points is simpler. For the purpose of automatically identifying the individual vessels and their main branches, the skeleton will be used as graph. The vertices of the graph will represent the ramification points in the skeleton and edges will represent connections between these points. For each edge the average vessel radius will be determined and saved as a property for the given edge, thus allowing us to distinguish between adjacent edges. The method used to search through the graph can be viewed in algorithm 3.

Algorithm 3 Automatic Determination of Vessel Branches using Graphs

1: {**INPUT: Graph** $G = (V, E)$ **with** V **representing ramifications and edges** E **connecting ramifications while storing the branch radius**}
2: **{OUTPUT: Graphs** $G_0 ... G_n$ **representing the different vessel system branches}**

3: $G_0 \leftarrow$ **largest edge** $\in G$**;**
4: $count = 1$; **{Number of branches}**
5: **for** $i = 0$ **to** $count$ **do**
6: **for all adjacent and unvisited edges** $\in G_i$ **do**
7: **Choose largest adjacent** $edge$**;**
8: **if** $edge > n*$ **next largest adjacent edge then**
9: $count++$;
10: **Start new Graph** G_{count};
11: $G_{count} \leftarrow edge$;
12: **else**
13: $G_i \leftarrow edge$;
14: **end if**
15: **Add connected Vertex to appropriate Graph** $G_{0..i}$
16: **end for**
17: **end for**

Algorithm 3 takes a graph G of vertices and edges, where each edge also stores its average radius, and outputs a set of acyclic directed graphs $G_0 ... G_i$, with each graph starting at the root of the hepatic vein, portal vein, or one of the branches or fragments thereof. The algorithm starts by picking the edge with the largest radius, which is usually the portal vein's entrance into the liver. It adds this edge to the initial graph G_0. Starting from here, the algorithm finds the next largest adjacent edge from the global graph G, that has not yet been visited.

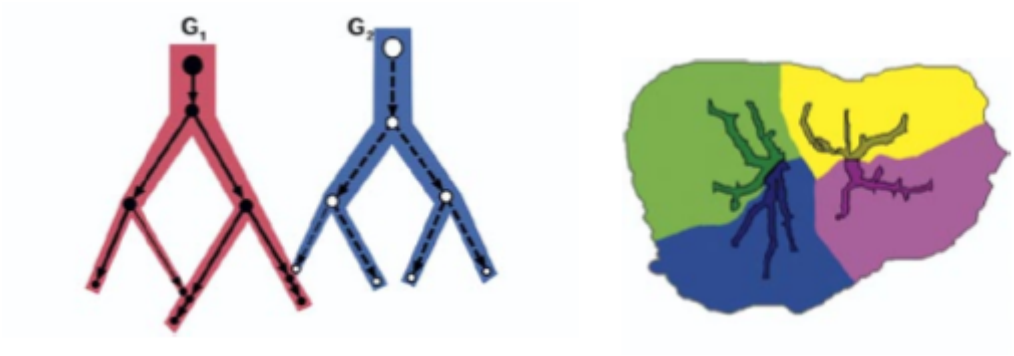

(a) (b)

Figure 3: The results of the graph based vessel flow estimation can be seen in (a), where two graphs are automatically separated, even in points where they cross, and in (b) the results of the automatic segment calculation.

To control how many branches are created, a special parameter $n \in]0 : \infty[$ is needed. The parameter is used to specify the factor that an adjacent edge's radius can increase. If this factor is exceeded, then a new graph is added G_1 and the edge is added as its root. Depending on the choice of n, either a large number graphs are created (small n), or only a single graph is created (large n). A value of 1 would for example mean that vessels would not be allowed to increase in size in a path from the root of a graph G_i to the periphery. The authors suggest that a value of 0.5 should be used, as that works well for most clinical data.

The end results of using these processing steps, is that the clinician will have the ability to access the structure of each individual vessel in the liver. The automatic determination of branches greatly helps in determining vascular areas, as well as discovering which vessels would be affected by a given resection plan.

2.2.3 Determination of Vascularization Areas

The final processing step necessary for planning the resection strategy is calculating the patient's liver segments, which is necessary to minimize the risk when estimating different approaches. Because of the limited spatial resolution of modern imaging modalities, not all branches of the hepatic and portal veins are able to be segmented.

We need to find a function that estimates the missing branches in our image, so that it can predict with a good amount of certainty for any given liver voxel what vascularization segment supports it. In particular what we are looking for is a function $g : L \rightarrow \{1, ..., n\}$ that maps voxels $v \in L$ to one of the liver segments, which in turn are supported by one of the branches B_i. This is far from a trivial task, and there are currently several methods available to accomplish this, each with its advantages and disadvantages. For this paper we will look at the simplest method for estimating the missing branch information and segmental anatomy, known as nearest neighbor segment approximation (NNSA).

Before the segment approximation can begin, the liver itself needs to be segmented in its entirety from the image, something that was not necessarily performed in one of the previous steps. This too is not a simple problem with a clear cut solution. The authors used an advanced hybrid segmentation process that is based upon statistical models of the liver [8].

Using their method the liver is automatically segmented based upon statistical models of the average contours and topology of the liver, derived from anatomical samples taken from over 30 different patients, which are then used as constraints in segmenting the patient's liver.

Nearest neighbor segment approximation is based on the idea that for any given voxel, the segment that the voxel belongs to is determined by the nearest vessel branch. In order to automatically calculate this property the following definitions are needed. The euclidean distance between each voxel v and each branch B_i is defined as

$$d_i(v) = \min_{v' \in B_i} \|v - v'\|^2 \text{ where } v \in L. \tag{1}$$

The liver voxels $v \in L$ are assigned to each branch as follows

$$\begin{aligned} g_{NNSA}(v) &= k \\ \text{where } d_k(v) &= \min\{d_1(v), ..., d_n(v)\}. \end{aligned} \tag{2}$$

The next criterion is used to define which liver voxels belonging which segment S_i

$$S_i = \{v \in L | g_{NNSA}(v) = i\}. \tag{3}$$

The result of applying the listed criteria is that each voxel is assigned to the segment with the branch that is nearest to it. This simple method provides surprisingly accurate segment distribution, that in turn dramatically helps in estimating the risk involved in the resection plans by discovering which liver sections are at risk for devascularization when a particular branch is removed. The surgeon can then interactively view the tumor metastases along with the anatomical segments where they lie.

3 Intraoperative Surgical Tools

3.1 Intraoperative Imaging

Ultrasonography is a time tested tool that is invaluable in liver resection procedures. In most operations it is used as the primary imaging modality used by the surgical team to guide their efforts [14]. In contrast to preoperative imaging, intraoperative images have to be continuously retaken, mostly because of organ motion that occurs during surgery. Some specialized centers include intraoperative CT or MR systems, but this provides certain prohibitive logistical problems for liver resections, aside from the cost. It was because of these factors that the authors decided to use three dimensional ultrasonography for their procedures.

Three dimensional ultrasonography is very similar to standard ultrasound machines, both use a probe that must be physically applied to the surface of the area that is visualized. The largest difference is that a three dimensional ultrasonography machine automatically rotates the probe around the target area, thus generating a connected three dimensional image, hence the name 3D ultrasonography.

3.2 Intraoperative Navigation

The preoperative image processing techniques discussed in the previous section allow for detailed planning and simulation of the liver resection, before the patient even enters the

Figure 4: This shows a portion of the intraoperative navigation display. The ultrasound slices are displayed as well as the preoperative liver vascularization model.

operating room. Nonetheless, these preoperative plans and models are not directly applicable in the procedure, mostly because the organ shifts its position in the body during the surgery. Any form of navigated surgery based entirely on these images and plans would be highly inaccurate.

The authors have implemented a solution to this problem by using intraoperative ultrasonography in combination with a tracked navigation system. By providing tools for precisely measuring the distance and orientation between surgical tools and major anatomical landmarks, such as hepatic and portal vein branches or the tumor site, the overall risk of greatly deviating from the preoperative plan is reduced. The task of transferring the preoperative plan no longer needs to be carried out solely by the spatial orientation capabilities of the surgical team.

The general setup was fairly similar to most common navigation environments used in other types of surgery [5]. Each surgical instrument was fitted with retroreflective spheres, as was the ultrasonography probe. An Infrared tracking camera was installed in the operating room for the purpose of tracking all of the surgical instruments and the ultrasonography probe, meaning that a free line of sight had to be kept between the tracked objects and the camera at all times. Because the probe was calibrated preoperatively, the 3D ultrasound image and the surgical instruments were all able to be mapped into the same coordinate system.

The surgeries began by mobilizing and exposing the liver surface. The position and orientation of the surgical instrument was visualized inside the registered ultrasound image. The navigation display was split into two section planes, the coronal plane which was in line with the probe, and the axial plane at a right angle to it, mostly in alignment with the transverse

direction. The two planes intersection level is displayed in both slice views. The tumor sites and major blood vessels were displayed in contrast enhancing colors on the monitor, see figure 4.

While navigating the surgical instrument over the surface of the liver, the mean distances to major blood vessels was automatically calculated by the system. When the surgical team had determined the correct resection entry plane, the coronal plane is fixed to the tip of the surgical instrument, and the transverse plane is fixed to the level of the tumor. This helps the surgeon then accurately guide the instrument around the tumor and the major vessels.

4 Experiments and Results

An experiment was conducted using the methods described in the previous sections, and compared with a historical control group operated on by the same surgical team. A total of 89 patients were considered for navigated liver resection, of which 55 had tumors that were superficially located at or near the surface. The remaining 34 patients had tumors that were located more centrally near the major vessels and were selected for the procedure. One patient was excluded on operation due to peritoneal carcinomatosis, a condition where the abdominal cavity lining contains metastases. One additional patient was excluded because the the reflective spheres could not be attached to the ultrasound device. In total 32 patients underwent navigated resections.

Mean operating time was comparable when contrasted with conventional resection, with the navigated variation lasting 290 min, and the conventional 285 min. The mean blood loss was 700 ml for the navigated surgery, and 960 for conventional. The number of resections with a negative margin R0 was 30 for the navigated, and 28 for the non navigated. The average R0 margin was 8 mm for the navigated resection, and 9mm for the non navigated. In the navigated procedure 6 patients had post-operative complications, whereas 5 had complications with the conventional method. In general, one additional person was needed to operate the navigation equipment, and mean navigation time was 25 min.

5 Conclusion

Computer based image processing and navigation methods present a great benefit to liver resection procedures. Not only is the pre-operative planning massively enhanced, when compared with classical methods, but also the overall surgical precision is increased. The problems due to the lack of high precision tools can be directly measured in statistics associated with liver resections, where positive resection margins still have high occurrence, even in specialized centers. Navigation in combination with sophisticated preoperative planning presents itself as a way to guarantee an increased amount of reproducibility amongst the operations, that in turn should have a positive effect on the outcome of the patients involved. The direct benefit of using such modern methods should dramatically outweigh the increased costs involved.

Further improvements can be made by more actively combining the preoperative surgical plan with the intraoperative navigation display [10]. Several of the authors have already proposed and tested methods for registering three dimensional ultrasound data sets to pre-operative CT images. This would in effect move the burden of transferring the preoperative plan to the navigation display from the surgeon to a computer, in this case adding another layer of reproducibility to the procedure.

References

[1] Efthimios A. Bakalakos, Julian A. Kim, Donn C. Young, and Edward W. Martin Jr. Determinants of survival following hepatic resection for metastatic colorectal cancer. *World Journal of Surgery*, 22(4):399–405, April 1998.

[2] S. Beller, M. Hhnerbein, T. Lange, S. Eulenstein, B. Gebrauer, and P. M. Schlag. Image-guided surgery of liver metastases by three-dimensional ultrasound-based optoelectronic navigation. *British Journal of Surgery*, (94):866–875, March 2006.

[3] C. Couinaud. *Le foie, etudes anatomiques et chirurgicales.* Masson, 1957.

[4] Yuman Fong, Joseph Fortner, Ruth L. Sun, Murray F. Brennan, and Leslie H. Blumgart. Clinical score for predicting recurrence after hepatic resection for metastatic colorectal cancer. *Annals of Surgery*, 230(3):309–321, september 1999.

[5] P. Grunert, K. Darabi, J. Espinosa, and R. Filippi. Computer-aided navigation in neurosurgery. *Neurosurg Rev*, 26:73–99, 2003.

[6] R.M. Hansen, L. Ryan, T. Anderson, B. Krzywda, E. Quebbeman, A. Benson, D.G. Haller III, and D. C. Tormey. Phase iii study of bolus versus infusion flourouracil with or without cisplatin in advanced colorectal cancer. *Journal of the National Cancer Institut*, 88:668, 1996.

[7] V. Kumar, N. Fausto, and A. Abbas. *Robins and Cotran Pathologic Basis of Disease.* Saunders, 7th edition, 2003.

[8] H Lamecker, T Lange, M Seebass, Eulenstein S, Westerhoff M, and HC Hege. Automatic segmentation of the liver for the preoperative planning of resections. *Medicine meets virtual reality 11*, pages 171–174, 2003.

[9] Hauke Lang, Arnold Radtke, Milo Hindennach, Tobias Schroeder, Nils R. Frhauf, Massimo Malag, Holger Bourquain, Heinz-Otto Peitgen, Karl J. Oldhafer, and Christoph E. Broelsch. Impact of virtual tumor resection and computer-assisted risk analysis on operation planning and intraoperative strategy in major hepatic resection. *Arch Surg*, 140:629–638, July 2005.

[10] Thomas Lange, Sebastian Eulenstein, Michael Hhnerbein, Hans Lamecker, and Pter-Michael Schlag. *Augmenting Intraoperative 3D Ultrasound with Preoperative Models for Navigation in Liver Surgery*, pages 534 – 541. Medical Image Computing and Computer-Assisted Intervention. Springer Berlin, 2004.

[11] T. C. Lee, R. L. Kashyap, and C. N. Chu. Building skeleton models via 3-d medial surface/axis thinning algorithms. *Graphical Models Image processing*, 56(6):462–478, 1994.

[12] Dirk Selle, Bernhard Preim, Andrea Schenk, and Heinz Otto Peitgen. Analysis of vasculature for liver surgical planning. *IEEE Transactions on Medical Imaging*, 21(11):1344 – 1357, November 2002.

[13] JN Vauthey, A Chaoui, KA Do, and et al. Standardized measurement of the future liver remnant prior to extended liver resection. *Surgery*, 127:512 – 519, 2000.

[14] Johannes Zacherl, Christian Scheuba, Martin Imhof, Maximilian Zacherl, Friedrich Lngele, Peter Pokieser, Fritz Wrba, Etienne Wenzl, Ferdinand Mhlbacher, and Raimund Jakesz an Rudolph Steininger. Current value of intraoperative sonography during surgery for hepatic neoplasms. *World Journal of Surgery*, 26:550–554, 2002.